Simulations of Atmospheric General Circulations of Earth-like Planets by AFES

Project Representative

Yoshi-Yuki Hayashi   Department of Earth and Planetary Sciences, Kobe University

Authors

Yoshi-Yuki Hayashi[*1], Masaki Ishiwatari[*2], Masatsugu Odaka[*2], Yuuji Kitamura[*3], Masahiro Takagi[*4], Yoshiyuki O. Takahashi[*1], Shinichi Takehiro[*5], Kensuke Nakajima[*6], George L. Hashimoto[*7] and Yoshihisa Matsuda[*8]

*1 Department of Earth and Planetary Sciences, Kobe University

*2 Department of Cosmosciences, Hokkaido University

*3 Meteorological Research Institute

*4 Department of Earth and Planetary Science, The University of Tokyo

*5 Research Institute for Mathematical Sciences, Kyoto University

*6 Department of Earth and Planetary Sciences, Kyushu University

*7 Department of Earth Sciences, Okayama University

*8 Faculty of Education, Tokyo Gakugei University

High resolution simulations of the Martian atmosphere have been performed by using a General Circulation Model (GCM) based on the AFES (Atmospheric GCM for the Earth Simulator). Also performed is a low resolution simulation of the Venus atmosphere by using a simplified GCM but with an accurate radiation model for the Venus atmosphere as a preparation for high resolution simulation. Our aim is to have insights into the dynamical features of small and medium scale disturbances in the Earth-like atmospheres and their roles in the general circulations. Mars simulations are performed by the use of quite high horizontal resolution which is almost the applicable limit of hydrostatic approximation. The results of the simulations show a variety of small scale disturbances. Dust mass flux shows that small scale disturbances contribute dust lifting significantly. Dust mass flux increases as the increase of horizontal resolution. It is shown that the horizontal scale of small scale disturbances in the low latitude decreases as the increase of resolution. As for the simulation of the Venus atmosphere, zonal wind remains very weak especially below 50 km even with the use of an accurate radiation model, although the result shows mean wind with remarkable jet above 50 km. This result supports the result of the previous study that the Gierasch mechanisms may not work in the lower Venus atmosphere.

Keywords: planetary atmospheres, superrotation, dust storm, Earth, Mars, Venus

1. Introduction

The structure of the general circulation differs significantly with each planetary atmosphere. For instance, the atmospheres of the slowly rotating Venus and Titan exemplify the superrotation, while the weak equatorial easterly and the strong mid-latitude westerly jets are formed in the Earth's troposphere. The global dust storm occurs in some years on Mars, but a similar storm does not exist in the Earth's atmosphere. Understanding physical mechanisms causing such a variety of structures of the general circulations of planetary atmospheres is one of the most interesting and important open questions of the atmospheric science and fluid dynamics.

The aim of this study is to understand the dynamical processes that characterize the structure of each planetary atmosphere by simulating circulations of those planetary atmospheres by using general circulation models with the common dynamical core of the AFES [1]. Appropriate physical processes are adopted for each planetary atmosphere. In our project so far, we have been mainly performing simulations under the condition of Mars. In addition, the accurate radiation model of the Venus atmosphere has been constructed toward performing simulations under the condition of Venus. In the followings, the particular targets of each simulation, the physical processes utilized, and the results obtained will be described briefly.

2. Mars simulation

2.1 Targets of simulations

Dust suspended in the Martian atmosphere plays an important role to maintain thermal and circulation structure of the Martian atmosphere through radiative process. However, the physical mechanisms of dust lifting are not understood fully. A previous study by using a Mars GCM [2] suggests that the effects of wind fluctuations caused by small and medium scale disturbances would be important for the dust lifting processes. However, the features of small and medium scale disturbances which may contribute to the dust lifting have not been clarified. Disturbances of these scales are not in the range of observations. In order to examine the disturbances in the Martian atmosphere and its effects on dust lifting, we have been performing medium and high resolution simulations of Martian atmosphere by using a Mars GCM. In this fiscal year, simulations are continued with the resolution increased up to almost the applicable limit of hydrostatic approximation.

2.2 Physical processes

The physical processes used for the Mars simulations are introduced from the Mars GCM [3,4] which has been developed in our group so far. The implemented physical processes are the radiative, the turbulent mixing, and the surface processes. By the use of this GCM, the simulations in northern fall condition are performed. Resolutions of simulations are T79L96, T159L96, T319L96, and T639L96, which are equivalent to about 89, 44, 22, and 11 km horizontal grid sizes, respectively. The T639L96 simulation is the highest resolution simulation of Martian global atmosphere that have been performed ever in the world, and this resolution is almost the applicable limit of hydrostatic approximation. In the simulation performed in this fiscal year, the atmospheric dust distribution is prescribed, and the dust is uniformly distributed in horizontal direction with an amount corresponding to visible optical depth of 0.2. But, the dust lifting parameterization [5] is included in the model, and the possibility of dust lifting can be diagnosed. As the

surface condition, the observed spatial variations of orography, surface albedo, and surface thermal inertia are prescribed. As a sensitivity test, the simulations with flat surface, uniform albedo and thermal inertia, are also performed to examine effects of such variations and intrinsic effects of horizontal resolution on disturbance generation and dust lifting.

2.3 Results

Figure 1 shows a snapshot of global distribution of relative vorticity at the 4 hPa pressure level at northern fall obtained from T639L96 simulation. In the simulation, a variety of atmospheric disturbances can be observed, such as baroclinic waves in the northern middle and high latitudes, vortices and shear lines in the lees of mountains, small scale streaks, and small scale vortices in the low latitude. Here, the small scale vortices in low latitude are focused. By comparing the vorticity distributions of different resolution simulations (Fig. 2), it is found that the horizontal size of these vortices decreases with increasing horizontal resolution. It does not seem to converge up to the highest resolution performed in our study. Further, those vortices develops in earlier local solar time in high resolution simulation than that in lower resolution ones. It is considered that these small scale vortices are generated by convective motion represented in the model. Although thermal convection is too small to be resolved fully in the model, the higher resolution model represents those better than lower resolution model.

In order to assess the effects of small and medium scale disturbances on dust lifting, the resolution dependence of globally integrated dust mass flux diagnosed in the model is examined. Figure 3 shows the resolution dependence of globally integrated dust mass flux. The dust mass fluxes in the flat/uniform experiments are also shown. The globally integrated dust mass flux increases with increasing resolution significantly. This indicates that the small scale disturbances represented in high resolution simulations contribute dust lifting. However, the dust mass flux does not converge up to the
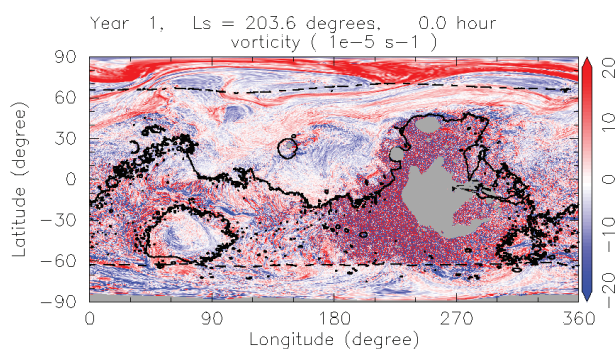

Fig. 1 Global distribution of vorticity at the 4 hPa pressure level at northern fall with the resolution of T639L96. Unit of vorticity is 10^{-5} s^{-1}. Also shown is the areoid (solid line) and low latitude polar cap edge (dashed line). Gray areas represent mountains at the 4 hPa pressure level.
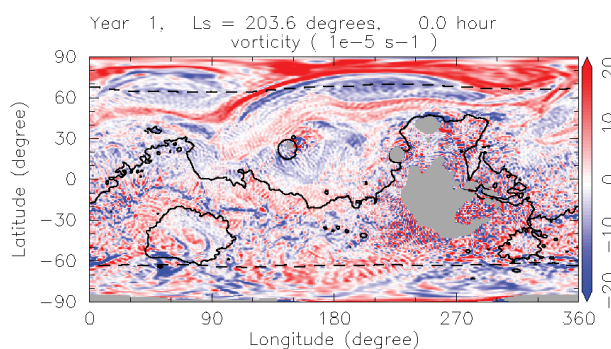
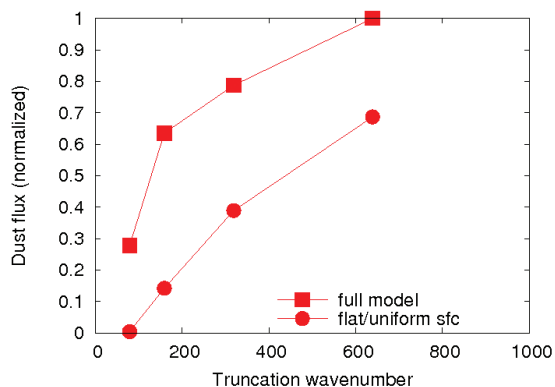Fig. 2 Same as Fig. 1, but with the resolution of T159L96.

Fig. 3　Resolution dependence of normalized globally integrated dust mass flux.

highest resolution performed in our study. This implies that the disturbances whose horizontal scale is smaller than about 10 km also contribute to dust lifting. At the same time, dust mass flux is larger in simulations with surface property variations than that in simulations with flat/uniform surface property. This clearly shows that the orography-related disturbances contribute significantly in dust lifting.

3. Venus simulation

3.1　Targets of simulations

The atmospheric superrotation is one of the most remarkable features of the Venus atmosphere. In recent years, several numerical experiments with GCMs have been performed to investigate the generation mechanism of the Venus atmospheric superrotation [6,7,8,9,10]. The results suggest that the Gierasch mechanism and the thermal tide mechanism may explain the atmospheric superrotation in dynamically consistent ways. However, in those studies, the radiative process is extremely simplified by Newtonian cooling. Since the Venus atmosphere is optically very thick, this simplification cannot be justified at

all, especially in the Venus lower atmosphere. It has been also pointed out that only extremely weak atmospheric superrotation is generated when realistic solar heating is adopted [9]. The results imply that the Gierasch mechanism may not work in the Venus lower atmosphere.

In order to understand the real generation mechanism of the atmospheric superrotation, an accurate radiation model has been developed. In this fiscal year, we started to perform preliminary simulations of the Venus atmosphere by implementing the developed radiation model into a low resolution GCM.

3.2　Model

In our Venus simulation, a low resolution spectral model, which is different from the AFES and can be easily performed also on a desktop computer, is used as a preparation for high resolution simulations. The resolution is T10L50, whose vertical domain extends from the ground to about 100 km with almost the constant grid spacing of 2 km. The model includes vertical and horizontal diffusion. Coefficients of vertical eddy viscosity and heat diffusion are set to 0.1 $m^2 s^{-1}$ and 0.01 $m^2 s^{-1}$, respectively. Horizontal eddy viscosity is represented by the second-order hyperviscosity with relaxation time of 1 Earth day for the maximum wave number component. Unlike the many previous studies, Rayleigh friction (or sponge layer) is not used in the present model except at the lowest level, where the surface friction acts on horizontal winds. In addition, the dry convective adjustment scheme is used to restore the temperature lapse rate to the neutral one when an atmospheric layer becomes statically unstable.

The solar heating is zonally averaged and prescribed in the present study. The vertical profile is based on the works of Tomasko et al. [11] and Crisp [12]. It is noted that the solar heating is artificially attenuated above 80 km. This does not affect general circulation in the lower atmosphere on which we
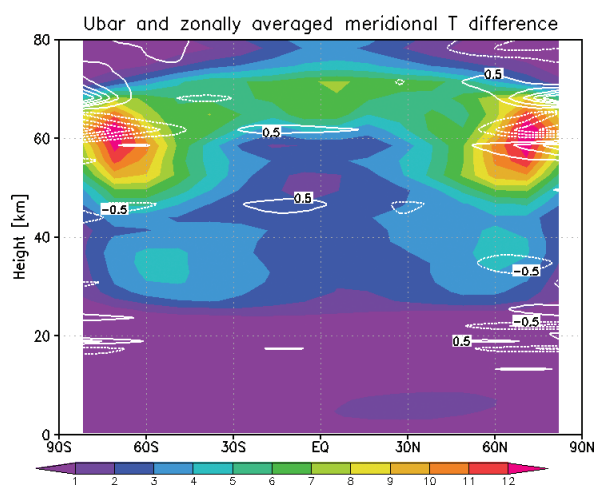

Fig. 4　Distribution of mean zonal flow obtained for RT case at 10th Earth year. Color shade and white contours indicate velocity of the mean zonal flow (m s⁻¹) and zonally averaged meridional temperature deviation (K), respectively.
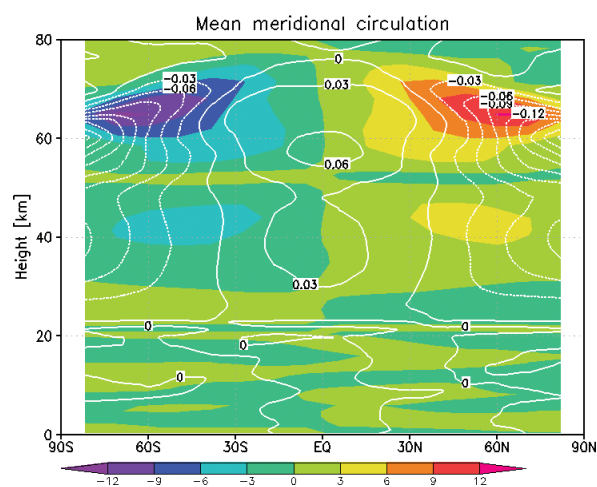

Fig. 5　Mean meridional circulation obtained for the RT case at 10th Earth year. Color shade and white contours indicate velocity of the mean meridional and vertical flows (m s⁻¹), respectively.

are focusing. The infrared radiation model is based on Takagi et al. [13]. The spectral range is 0-6000 cm^{-1}, which is divided into 10 channels. One-dimensional radiative and radiative-convective equilibrium temperature profiles obtained by this radiation model are in good agreement with observations [13].

In order to compare our results with those of a previous study [9], simulations with Newtonian cooling are also carried out. Vertical distribution of the relaxation time due to Newtonian cooling is taken from Takagi and Matsuda [7].

The initial state for time integration is an atmosphere at rest. Vertical profile of the initial temperature is taken from the VIRA [14]. It is also assumed that the initial temperature is horizontally uniform.

3.3 Results

Distribution of mean zonal flow obtained by the GCM with the infrared radiation model (hereafter referred to as RT) at 10th Earth year is shown in Fig. 4. The mean zonal flow with remarkable jets is generated in 30-70 km. The maximum velocity is about 11 m s^{-1} at about 70°N/S at 60 km, which is much less than observed values. Meridional temperature difference is only few K near the cloud top level. This is consistent with the weak zonal flows obtained in this simulation in view of thermal wind balance. A weak local maximum (7-8 m s^{-1}) is observed in the equatorial region at 70 km. Weaker midlatitude jets are also found at about 40 km. Below 30 km, the mean zonal flow remains very weak. The temperature contrast between the equator and poles is less than 1 K in this region.

The mean meridional circulation obtained for the RT case at 10th Earth year is shown in Fig. 5. It is clearly shown that the mean meridional circulation splits into two cells which extend from 20 to 50 km and from 50 to 80 km. The maximum velocity of the mean meridional flow is about 12 m s^{-1} at about 67 km near 60°N/S. Below 20 km, the mean meridional circulation is very weak. Static stability (defined by $dT/dz+g/C_p$) below 20 km is about 0.5 K km^{-1}, which seems consistent with observed values. It should be noted that the one-dimensional radiative

equilibrium temperature profile is statically unstable in the lower atmosphere [13]. This result suggests that the lower atmosphere is stabilized by the heat transfer associated with the horizontal convection (meridional circulation) in the lowest layer.

Figure 6 shows the distribution of the mean zonal flow obtained for a simulation with Newtonian cooling (hereafter referred to as NC) at 100th Earth year. The generated mean zonal flow is much faster than that obtained in the RT case. Velocities are about 30 and 45 m s^{-1} at the equator and 65°N/S at 65 km, respectively. The meridional gradient of temperature much increases in the polar regions at 50-60 km levels. Below 50 km, the mean zonal flow remains very weak, as in the RT case. The mean meridional circulation is shown in Fig. 7. A remarkable mean meridional cell can be observed in 50-75 km only. The maximum velocity of the mean meridional flow is about 10 m s^{-1} near 65 km. Below 50 km, the mean meridional circulation remains very weak in the NC case.

These results imply that the large meridional circulation extending from the ground to the cloud top level shown in the previous studies should be attributed to unrealistically strong solar heating used in their simulations. These results also support the idea that the Gierasch mechanism may not work in the lower Venus atmosphere. We will try to perform high resolution Venus simulation to examine the effects of small scale waves on generation of superrotation.

References

[1] Ohfuchi, W., H. Nakamura, M. K. Yoshioka, T. Enomoto, K. Takaya, X. Peng, S. Yamane, T. Nishimura, Y. Kurihara, and K. Ninomiya, 10-km Mesh Meso-scale Resolving Simulations of the Global Atmosphere on the Earth Simulator - Preliminary Outcomes of AFES (AGCM for the Earth Simulator) -, Journal of the Earth Simulator, 1, 8, 2004.

[2] Wilson, R. J. and K. Hamilton, Comprehensive Model Simulation of Thermal Tides in the Martian Atmosphere, J. Atmos. Sci., 53, 1290-1326, 1996.
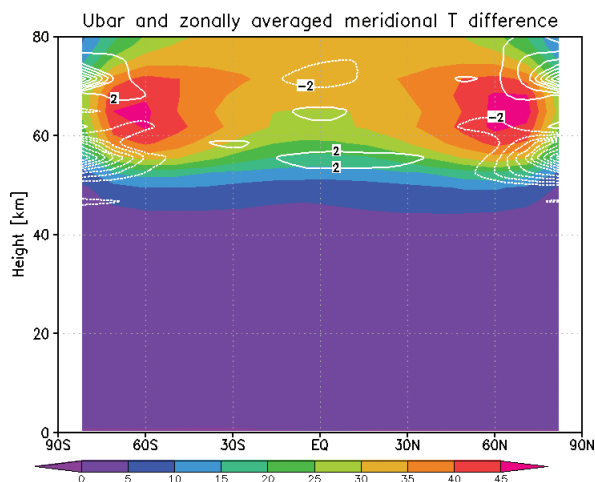
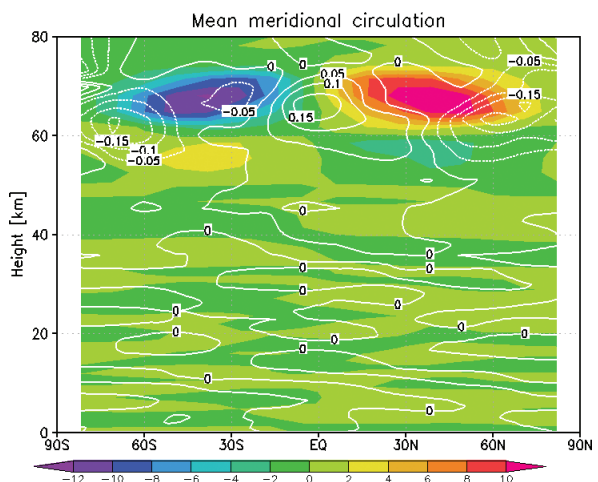Fig. 6 As in Fig. 4, but for the NC case at 100th Earth year.

Fig. 7 As in Fig. 5, but for the NC case at 100th Earth year.

[3] Takahashi, Y. O., H. Fujiwara, H. Fukunishi, M. Odaka, Y.-Y. Hayashi, and S. Watanabe, Topographically induced north-south asymmetry of the meridional circulation in the Martian atmosphere, J. Geophys. Res., 108, 5018, doi:10.1029/2001JE001638, 2003.

[4] Takahashi, Y. O., H. Fujiwara, and H. Fukunishi, Vertical and latitudinal structure of the migrating diurnal tide in the Martian atmosphere: Numerical investigations, J. Geophys. Res., 111, E01003, doi:10.1029/2005JE002543, 2006.

[5] Newman, C. E., S. R. Lewis, and P. L. Read, Modeling the Martian dust cycle 1. Representation of dust transport processes, J. Geophys. Res, 107, 5123, doi:10.1029/2002JE001910, 2002.

[6] Yamamoto, M and M. Takahashi, Dynamics of Venus' superrotation: The eddy momentum transport processes newly found in a GCM, Geophys. Res. Lett., 31, L09701,doi:10.1029/2004GLO19518, 2004.

[7] Takagi, M and Y. Matsuda, Effects of thermal tides on the Venus atmospheric superrotation, J. Geophys. Res., 112, D09112, doi:10.1029/2006JD007901, 2007.

[8] Lee, C., S. R. Lewis, and P. L. Read, Superrotation in a Venus general circulation model, J. Geophys. Res., 112, E04S11, doi:10.1029/2006JE002874, 2007.

[9] Hollingsworth, J. L., R. E. Young, G. Schubert, C. Covey, and A. S. Grossman, A simple-physics global circulation model for Venus: Sensitivity assessments of atmospheric superrotation, Geophys. Res. Lett., 34, L05202, doi:10.1029/2006GL028567, 2007.

[10] Kido, A and Y. Wakata, Multiple equilibrium states appearing in a Venus-like atmospheric general circulation model, J. Meter. Soc. Japan, 86, 969-979, 2008.

[11] Tomasko, M. G., L. R. Doose, P. H. Smith, and A. P. Odell, Measurements of the flux of sunlight in the atmosphere of Venus, J. Geophys. Res., 85, 8167-8186, 1980.

[12] Crisp, D., Radiative forcing of the Venus mesosphere: I. solar fluxes and heating rates, Icarus. 67, 484-514, 1986.

[13] Takagi, M., K, Suzuki., H, Sagawa., P, Baron., J, Mendrok., Y, Kasai., and Y, Matsuda., Influence of CO_2 line profiles on radiative and radiative-convective equilibrium states of the Venus lower atmosphere, J. Geophys. Res. 115, E06014, doi:10.1029/2009JE003488, 2010.

[14] Seiff, A., J.T, Schofield., A.J, Kliore., F.W, Taylor., S.S, Limaye., H.E, Revercomb., L.A, Sromovsky., V.V, Kerzhanovich., V.I, Moroz., and M. Ya, Marov., Models of the structure of the atmosphere of Venus from the surface to 100 kilometers altitude. Adv. Space Res. 5(11), 3-58, 1985.

AFES を用いた地球型惑星の大気大循環シミュレーション

プロジェクト責任者

林　　祥介　　神戸大学　大学院理学研究科

著者

林　　祥介 [*1]，石渡　正樹 [*2]，小高　正嗣 [*2]，北村　祐二 [*3]，高木　征弘 [*4]，高橋　芳幸 [*1]，
竹広　真一 [*5]，中島　健介 [*6]，はしもとじょーじ [*7]，松田　佳久 [*8]

*1　神戸大学　大学院理学研究科

*2　北海道大学　大学院理学研究院

*3　気象庁　気象研究部

*4　東京大学　大学院理学系研究科

*5　京都大学　数理解析研究所

*6　九州大学　大学院理学研究院

*7　岡山大学　大学院自然科学研究科

*8　東京学芸大学　教育学部

　大気大循環モデル AFES（AGCM（Atmospheric General Circulation Model）for the Earth Simulator）に基づく GCM を用いて、火星大気の高解像度大気大循環シミュレーションを実施した。加えて、今後の高解像度シミュレーションへの準備として、これまでに開発してきた高精度の金星大気放射モデルを用いて、低解像度での大気大循環シミュレーションを実施した。我々の研究の目的は、地球型惑星大気における中小規模擾乱の力学的特徴と、その大気大循環への影響を調べることである。火星大気シミュレーションは、おおよそ静水圧近似が成り立つ限界付近の非常に高い解像度で実施した。シミュレーションの結果は、様々な小規模擾乱を示している。小規模擾乱はダスト巻き上げに重要な寄与をしていることが示された。水平解像度の向上とともにダスト巻き上げ量が増加する。低緯度における小規模擾乱の水平スケールは解像度に依存していることも示された。また、金星大気シミュレーションに関しては、50 km 以上の高度においてジェットを伴う平均風を示しているが、高精度の放射モデルを用いているにも関わらず、特に 50 km 以下の高度では非常に弱い平均風しか形成されないことを示した。 この結果は、金星の下層大気においては、Gierasch メカニズムが働かないとする過去の研究と整合的である。

キーワード：惑星大気, スーパーローテーション, ダストストーム, 地球, 火星, 金星